MOLECULAR AND CELLULAR BIOLOGY, Feb. 1995, p. 932–942 Vol. 15, No. 2
0270-7306/95/$04.00+0

Activation-Induced T-Cell Death Is Cell Cycle Dependent and Regulated by Cyclin B†‡

RATI FOTEDAR,[1]* JODY FLATT,[2] SUNITA GUPTA,[1] ROBERT L. MARGOLIS,[1] PATRICK FITZGERALD,[2] HELEN MESSIER,[2] AND ARUN FOTEDAR[2]*

Institut de Biologie Structurale J.-P. Ebel, 38027 Grenoble Cedex 1, France,[1] and Division of Molecular Biology, La Jolla Institute for Allergy and Immunology, La Jolla, California 92037[2]

Received 25 July 1994/Returned for modification 15 September 1994/Accepted 3 November 1994

Developing thymocytes and some T-cell hybridomas undergo activation-dependent programmed cell death. Although recent studies have identified some critical regulators in programmed cell death, the role of cell cycle regulation in activation-induced cell death in T cells has not been addressed. We demonstrate that synchronized T-cell hybridomas, irrespective of the point in the cell cycle at which they are activated, stop cycling shortly after they reach G_2/M. These cells exhibit the diagnostic characteristics of apoptotic cell death. Although $p34^{cdc2}$ levels are not perturbed after activation of synchronously cycling T cells, cyclin B- and $p34^{cdc2}$-associated histone H1 kinase activity is persistently elevated. This activation-dependent induction of H1 kinase activity in T cells is associated with a decrease in the phosphotyrosine content of $p34^{cdc2}$. We also demonstrate that transient inappropriate coexpression of cyclin B with $p34^{cdc2}$ induces DNA fragmentation in a heterologous cell type. Finally, in T cells, cyclin B-specific antisense oligonucleotides suppress activation-induced cell death but not cell death induced by exposure to dexamethasone. We therefore conclude that a persistent elevation of the level of cyclin B kinase is required for activation-induced programmed T-cell death.

Programmed cell death (apoptosis) is a highly regulated physiological process by which specific cells are eliminated from an organism. The phenomenon of programmed cell death is associated with pronounced cellular changes exemplified by the generation of oligonucleosomal DNA ladders, dissolution of the nuclear membrane, hypercondensed pycnotic nuclei, and cytoplasmic blebbing (50). Recent studies have identified a number of positive and negative regulators of cell death (5, 9, 19, 20, 24, 30, 42, 49, 51), suggesting the existence of multiple cell death pathways. Tumor suppressor gene p53 null mice remain susceptible to activation-induced cell death, but radiation-induced cell death is severely impaired (5). Genetic analysis of *Caenorhabditis elegans* has demonstrated that the *ced-3* gene, which is related to the gene encoding the interleukin-1β-converting enzyme in mammals, is required for physiological cell death (51). In contrast to Ced-3, Ced-9 (19) and its human homolog Bcl-2 (20) block apoptotic cell death. It has been suggested that Bcl-2 blocks death by heterodimerizing with proteins such as Bax which accelerate apoptosis (30). The roles of these proteins in different pathways leading to cell death await clarification of their function.

During T-cell development, autoreactive immature T cells in the thymus are deleted by activation-induced programmed cell death (41, 43, 45). A T-cell hybridoma A11 (10), which undergoes activation-induced cell death, has been used as a model system to clarify aspects of programmed cell death in T cells (42–44). A11 cells, like thymocytes, undergo programmed cell death and DNA fragmentation after activation via the T-cell receptor with anti-CD3 (2, 27, 41, 43–45). Cyclosporine abrogates anti-CD3-induced cell death in both A11 cells and thymocytes (2, 27, 43). In addition to anti-CD3, antigen, lectins, and phorbol esters plus ionophores induce programmed cell death in both immature thymocytes and T-cell hybridomas (21, 25, 27, 41, 43–45, 47). Furthermore, anti-CD3 inhibits growth of both transformed and nontransformed T cells (2, 4, 26, 27, 29, 48).

Studies on activation-induced cell death in T-cell hybridomas have revealed a critical role for c-*myc* in inducing cell death (42). Similarly, overexpression of c-*myc* has been shown to induce programmed cell death in serum-deprived rat fibroblast cells (9). Recently, the induction of nur77, an orphan steroid receptor, has been implicated in activation-induced death of T cells (24, 49). Although several regulators of cell death have been identified, the role of cell cycle control in activation-induced death of T cells has not been adequately addressed. Earlier reports on activation-induced death of T cells have described a growth arrest characterized by a loss of cells in the S phase (2, 27). In this report, we show that activation induced synchronized cycling A11 cells to stop cycling shortly after they reached G_2/M. Persistently elevated levels of $p34^{cdc2}$- and cyclin B-associated histone H1 kinase were found in T cells undergoing activation-induced cell death. We also show that cotransfection of cyclin B with $p34^{cdc2}$ induces cell death and DNA fragmentation and that cyclin B-specific antisense oligonucleotides suppresses activation-induced T-cell death.

MATERIALS AND METHODS

Generation of synchronously cycling A11 cells. Synchronously cycling populations of A11 cells (10), a murine T-cell hybridoma, were generated by blocking cells (3×10^9 cells at 5×10^5/ml) with aphidicolin (2 μg/ml) for 10 to 12 h in spinner flasks. Cells were released from the drug block for 2 to 3 h, and progression of the synchronous population into the S phase was monitored every 30 min by assaying the DNA content by flow cytometry. Synchronously cycling cells in the S phase were then collected by centrifugal elutriation. Synchronously cycling cells in G_2/M were obtained in a similar manner, by centrifugal elutriation

* Corresponding authors. Mailing address (R.F.): Institut de Biologie Structurale J.-P. Ebel, 41 avenue des Martyrs, 38027 Grenoble Cedex 1, France. Phone: 33 76 88 96 15. Fax: 33 76 88 54 94. Mailing address (A.F.): Division of Molecular Biology, La Jolla Institute for Allergy and Immunology, 11149 North Torrey Pines Rd., La Jolla, CA 92037. Phone: (619) 558-3542. Fax: (619) 558-3525.

† Publication 95 from the La Jolla Institute for Allergy and Immunology.

‡ A.F. dedicates this paper to the memory of the late Thomas Wegmann.

of A11 cells released from an aphidicolin block, and monitored by flow cytometry until the cells had a G_2/M DNA content. We also obtained synchronously cycling G_1 cells by centrifugal elutriation of an asynchronous population of A11 cells. Approximately 15% of these G_1 cells did not cycle, while the rest of the population cycled synchronously. Synchronous populations of A11 cells at different phases of the cell cycle were activated with concanavalin A (ConA) or with immobilized anti-CD3 antibody (3) as described elsewhere (43).

Cell cycle analysis. The DNA content of the cells was determined by propidium iodide staining (34). DNA synthesis was determined by bromodeoxyuridine incorporation into DNA (34). In brief, 5×10^5 cells were incubated with 10 μM bromodeoxyuridine (Sigma) for 30 min at 37°C. The cells were washed, fixed with 70% ethanol, and incubated with 2 N HCl–0.5% Triton X-100 at room temperature for 30 min. After neutralization with 0.1 M $Na_2B_4O_7$ (pH 8.5), the cells were resuspended in 50 μl of phosphate-buffered saline (PBS) containing 1% bovine serum albumin (BSA), 0.5% (vol/vol) Tween 20, and 20 μl of anti-bromodeoxyuridine–fluorescein isothiocyanate antibody (Becton Dickinson) and incubated for 30 min at room temperature. Finally, the cells were resuspended in 1 ml of PBS containing 5 μg of propidium iodide (Sigma) per ml.

DNA fragmentation. Induction of DNA strand breaks after T-cell activation was determined by measuring terminal transferase-dependent incorporation of dUTP as described previously (15). In brief, cells were fixed with paraformaldehyde, washed, and incubated at 37°C for 30 min in 50 μl of 0.2 M potassium cacodylate–25 mM Tris (pH 6.6)–2.5 mM $CoCl_2$–0.25 mg of BSA per ml–10 μM biotin-16-dUTP–100 U of terminal transferase (Boehringer Mannheim) per ml. After being washed, cells were incubated in the dark in 100 μl of 0.6 M NaCl–0.06 M sodium citrate–2.5 μg of fluoresceinated avidin (Sigma) per ml–0.1% Triton X-100–5% (wt/vol) nonfat dry milk. The cells were washed in PBS containing 0.1% Triton X-100 and resuspended in 1 ml of PBS containing 5 μg of propidium iodide per ml and 0.1% RNase A (Sigma). Samples were analyzed by using excitation at 488 nm and the 525-nm BP filter for green (fluorescein isothiocyanate) and the 620-nm LP filter for red (propidium iodide) fluorescence on a Becton-Dickinson FACScan. Data were collected with the FACScan Research program and analyzed with the Becton Dickinson LysysII program. This method of assaying DNA strand breaks directly determines the percentage of cells undergoing DNA strand breaks and the relative severity of DNA strand breaks in individual cells. This method also allows early detection of DNA fragmentation before oligonucleosomal fragments can be detected on agarose gels.

Immunofluorescence. Cells were prepared for immunofluorescence analysis of chicken cyclin B as described previously (13). A11 cells were prepared for analysis of cyclin B and MPM-2 antigen as described previously (1), with the following modifications. For A11 cells, these procedures were adapted for suspension culture cells. Cells were fixed with 2% paraformaldehyde for 20 min at 37°C, spun on coverslips, and treated for 3 min with 0.2% Triton X-100 in PBS. The coverslips were washed with PBS and incubated for 1 h with the primary antibody diluted in PBS containing 3% BSA, 0.05% Tween 20, and 0.05% sodium azide. After being washed with PBS, coverslips were incubated with fluorescein isothiocyanate-labelled goat anti-rabbit or fluorescein isothiocyanate-labelled goat anti-mouse secondary antibody (Cappel) for 30 min at 37°C. After being washed, the coverslips were incubated with 1 μg of propidium iodide per ml for 3 min at room temperature, washed with PBS, and placed on a Dabco-glycerol drop on slides. For double staining, Texas red-labelled sheep anti-mouse antibody was used instead of propidium iodide. Cells were examined on a Nikon Optiphot microscope equipped for epifluorescence and phase-contrast microscopy. For quantitative analysis, images were collected with a Bio-Rad Confocal Imaging System.

Cell extracts. Synchronous populations of A11 cells were activated in the S phase, and extracts were prepared from both control unactivated and activated cells at the indicated times. Extracts were made from at least 2×10^8 cells, and aliquots from these preparations were used for immunoblots and protein kinase assays. To prepare extracts, cell pellets were washed twice with PBS and finally resuspended in an equal volume of hypotonic buffer (20 mM *N*-2-hydroxyethylpiperazine-*N*′-2-ethanesulfonic acid [HEPES; pH 7.5], 5 mM KCl, 1.5 mM $MgCl_2$, fresh 0.1 mM dithiothreitol) (11, 12). After 30 min on ice, the cells were homogenized and centrifuged at $10{,}000 \times g$ for 10 min at 4°C. NaCl was added to the supernatant to 0.1 M, and aliquots of the $100{,}000 \times g$ supernatant were stored at −80°C.

Antibodies. Affinity-purified rabbit polyclonal antibody, raised against the carboxy-terminal sequence (CDNQIKKM) of human $p34^{cdc2}$ (7), was obtained from Oncogene. The ability of this antibody to immunoprecipitate $p34^{cdc2}$ kinase activity was specifically inhibited by the antigenic peptide (synthesized at Howard Hughes Medical Institute, University of Washington, Seattle). This antibody also recognizes murine $p34^{cdc2}$ but does not display any cross-reactivity with purified human $p33^{cdc2}$ (kindly provided by D. Morgan, University of California San Francisco) on Western immunoblots (data not shown). The human cyclin B1-specific monoclonal antibody GNS1 (39) was purchased from Pharmingen. The cyclin A-specific rabbit polyclonal antiserum was raised against *Escherichia coli*-expressed human cyclin A (16) and kindly provided by M. Ohtsubo and J. Roberts (Fred Hutchinson Cancer Research Center). The specificity of the anti-cyclin A antibody was confirmed in immunoblot assays with recombinant cyclin proteins (data not shown). Monoclonal antibody specific for the MPM2 epitope was kindly provided by P. N. Rao (6), mouse anti-β-tubulin antibody was purchased from Sigma, and anti-lamin B-specific human autoimmune serum was kindly provided by J.-C. Courvalin (17). A phosphotyrosine-specific antibody, 4G10, was purchased from Upstate Biotechnology Inc.

Immunoblots. Protein (10 μg) was resolved by sodium dodecyl sulfate-polyacrylamide gel electrophoresis (SDS-PAGE) and immunoblotted as described previously (13, 22), with the following changes. After overnight incubation with primary antibody, filters were washed three times with wash buffer plus 0.5% Tween 20 and incubated with 1:5,000 goat anti-rabbit or goat anti-mouse horseradish peroxidase (Tago) for 1 h, and proteins were visualized by ECL (Amersham).

Immunoprecipitations. Cell extract (30 μg) was adjusted to 40 mM HEPES (pH 7.4), 8 mM $MgCl_2$, 100 mM NaCl, 0.5% Nonidet P-40, 1 μg of aprotonin per ml, and 1 μg of leupeptin per ml (IP buffer) and added to 10 μl of packed protein A-Sepharose (Sigma) that had been preincubated with the appropriate dilution of antibody for 1 h in IP buffer. After 1 h, the protein A-Sepharose was washed five times with IP buffer and the samples were used for Western blots. For kinase assays, protein A-Sepharose was washed three times with IP buffer and twice with kinase buffer (40 mM HEPES, 8 mM $MgCl_2$).

Histone H1 kinase assays. Kinase assays were performed with 18 μl of reaction mixture containing 40 mM HEPES, 8 mM $MgCl_2$, 166 μM ATP, 5 μCi of [γ-^{32}P]ATP (3,000 Ci/mmol; NEN), 4 μg of histone H1 (Boehringer), and 10 μl of packed protein A-Sepharose. After 20 min at 37°C, the reaction was stopped by addition of SDS sample buffer. The reaction mixture was loaded on SDS–12% polyacrylamide gels, stained with Coomassie brilliant blue, dried, and autoradiographed.

Phosphotyrosine content. The phosphotyrosine content of $p34^{cdc2}$ was determined by immunoprecipitating $p34^{cdc2}$ with anti-$p34^{cdc2}$ antibody and running the immunoprecipitates on denaturing polyacrylamide gels. The immunoblots were probed with a phosphotyrosine-specific antibody, 4G10, as described above, except that 2% gelatin (porcine skin; Sigma) was used to block nonspecific binding.

Transfection. The expression vectors of chicken $p34^{cdc2}$ and cyclin B2 (13, 22) under the control of the cytomegalovirus promoter and the chicken cyclin B2-specific antibody were the kind gifts of E. A. Nigg, Swiss Institute for Experimental Cancer Research, Epalinges, Switzerland. HeLa cells passaged for 24 h prior to use were transfected by the calcium phosphate protocol as described previously (13) with 5 μg of each expression vector per plate (made up to 10 μg of DNA per plate with pCMV vector DNA). The calcium phosphate precipitates were allowed to remain on the cells for 16 h, and the cells were analyzed 48 h after removal of the precipitates. The transfection efficiency was determined by staining adherent cells on coverslips for chicken cyclin B2 as described previously (13) and scoring positive cells by immunofluorescence microscopy. The control cells transfected with vector alone did not stain with the chicken cyclin B-specific antibody. The cell viability, DNA content, and DNA strand breaks of the transfected cells were determined as described previously (34). Plasmids were purified twice by centrifugation on equilibrium cesium chloride density gradients before transfection. Transient transfections with cyclin B and $p34^{cdc2}$, using CD20 as a transfection marker, were done in a human cervical carcinoma cell line, C33A. The CD20 expression plasmid was kindly made available to us by S. van den Heuvel and E. Harlow, Massachusetts General Hospital, Charlestown, Mass.; the CD20-specific antibody was purchased from Becton Dickinson; and C33A cells were obtained from the American Type Culture Collection.

Abrogation of cell death with cyclin B antisense oligonucleotides. The cyclin B1 antisense 5′ CATCGGGCTTGGAGAGGGATT 3′, a cyclin B1 sense 5′ AATCCCTCTCCAAGCCCGATG 3′, and control random phosphorothioate oligonucleotides were synthesized at Quality Controlled Biochemicals Inc., Hopkinton, Mass. A11 cells were activated with immobilized anti-CD3 monoclonal antibody 2C11 in the presence or absence of the appropriate oligonucleotide. The cell viability, DNA content, DNA strand breaks, and light-scattering characteristics of A11 cells were determined as described previously (34). Five different batches of cyclin B and control antisense oligonucleotides, synthesized at different times, gave identical results. The effect of cyclin B antisense oligonucleotide on cyclin B expression in A11 cells was determined by immunofluorescence microscopy with the GNS1 monoclonal antibody. The percentage of cyclin B-positive cells among A11 cells grown for 48 h in the presence of cyclin B antisense oligonucleotides was reduced from 37 to 7%. In contrast, ~30% of A11 cells grown with cyclin B sense or random control oligonucleotides were positive for cyclin B expression at that time. A similar reduction in the number of cyclin B-positive cells with cyclin B antisense but not cyclin B sense or random oligonucleotides was observed in three independent experiments.

RESULTS

Activation induces synchronously cycling T cells to stop cycling. To clarify the nature of the cell cycle perturbations induced by T-cell activation, we prepared synchronously cycling populations of A11 cells. A11 (10) is a T-cell hybridoma that undergoes activation induced cell death and has been extensively used to study programmed cell death in T cells (41–44). A11 cells were blocked with aphidicolin for 12 h and

then released from the drug block; synchronously cycling S phase cells were then obtained from this population by centrifugal elutriation. These cells were 100% viable and were capable of cycling synchronously from the S phase through another complete cell cycle. Synchronously cycling A11 cells in the S phase were activated with ConA or anti-CD3 antibodies (3). ConA and anti-CD3 antibodies both activate T-cell hybridomas to undergo activation-induced cell death (2, 27). We then tested for perturbations in cell cycle progression in activated T cells compared with unactivated cells. The control unactivated cells cycled synchronously through S, G_2/M, and G_1 phases and began to move into a second S phase by 14 h (Fig. 1A). In contrast, when activated cells entered G_2/M, cells with less than G_1 DNA content started to appear (Fig. 1A). The appearance of cells with less than G_1 DNA content is characteristic of apoptotic cell death (15). This population became more pronounced in activated cells at the time when control unactivated cells entered G_1 (Fig. 1A). The kinetics of the appearance of a population with less than G_1 DNA content after anti-CD3 activation were slower than in ConA-activated A11 cells (Fig. 1A). The exit from the cell cycle to apoptotic death in G_2/M is clearest for A11 cells activated with ConA. The presence of a transient G_1 peak after activation with anti-CD3 suggests that some of the activated cells might actually complete mitosis. An alternative explanation is that this peak represents G_2/M cells which have fragmented their DNA. If the latter is true, synchronously cycling cells activated in the S phase with anti-CD3 should not divide. We have directly examined this by determining total cell numbers at various times after activation of synchronously cycling S-phase cells with either ConA or immobilized anti-CD3 and comparing them with numbers of control unactivated cells. Figure 2C clearly shows that cell numbers in anti-CD3- or ConA-activated cultures did not double whereas unactivated cells doubled during the same period. Similar results were obtained when synchronously cycling cells were activated in G_1 (data not shown). The persistent elevation of cyclin B-associated kinase activity following anti-CD3 activation of A11 cells (see below) further supports our conclusion, since cells with high cyclin B-associated kinase activity cannot exit mitosis.

Activation of T cells in the S phase therefore induces cells to exit the cell cycle shortly after their arrival in G_2/M. If activation induces apoptosis in cycling cells after they reach G_2/M, activation of synchronously cycling cells in G_2/M should lead to a more rapid appearance of cells with less than G_1 DNA content than after activation in the S phase. Synchronously cycling cells in the S phase were obtained as described above. The cells were then allowed to cycle to G_2/M before activation. In five separate experiments, cells activated in G_2/M died faster (Fig. 1B) than did cells activated in S (Fig. 1A). The rapid appearance of A11 cells with less than G1 DNA content after 1 h of activation in G_2/M and the complete loss of cycling cells 3 h after activation in G_2/M strongly support our conclusion (Fig. 1B). We also obtained A11 cells in the S phase and the G_2/M phase by centrifugal elutriation of asynchronous A11 cells (not drug treated). Activation of such cells in G_2/M also induced death faster than that observed in similarly prepared cells which were activated in the S phase (data not shown).

To extend these observations, we also determined if activation of synchronously cycling A11 cells in G_1 induced them to stop cycling before or after reaching G_2/M. We obtained a synchronously cycling population in the G_1 phase by centrifugal elutriation of asynchronous A11 cells. In this population, ~15% of the cells do not cycle and the rest cycle synchronously. T cells activated in G_1 moved normally through G_1 and S, and cells with less than G_1 DNA content made their first appearance only after the population reached G_2/M (Fig. 1B). The control unactivated population continued to cycle. These data show that activation induces T cells to stop cycling after they reach G_2/M, irrespective of when cells are activated.

To determine if other indicators of apoptosis occur concurrently with the appearance of cells with less than G_1 DNA content, we monitored the cell viability, induction of DNA strand breaks, and apoptotic light-scattering characteristics in A11 cells activated in the S phase. Activation of synchronously cycling A11 cells in the S phase with either ConA or anti-CD3 induced a decrease in cell viability which parallels the appearance of cells with less than G_1 DNA content (Fig. 1A and 2A). Morphological changes in cells undergoing apoptosis are detectable by monitoring their light-scattering characteristics by flow cytometry. The characteristic decrease in cell size and the generation of apoptotic bodies are identifiable as a decrease in forward-angle light scatter (42, 46). The A11 cells with less than G_1 DNA content have a low forward-angle scatter characteristic of apoptotic T cells (Fig. 2B). The appearance of a population with a low forward-angle scatter after activation parallels the appearance of cells with less than G_1 DNA content. This suggests that the appearance of cells with less than G_1 DNA content after activation is coincident with cytoplasmic apoptotic changes in activated A11 cells. Activation of synchronously cycling A11 cells in the S phase also induced DNA strand breaks, diagnostic of apoptosis (15). DNA strand breaks, assayed by the terminal transferase assay, were induced in more than 75% of activated A11 cells compared with less than 1% of unactivated cells (Table 1). An increased incidence of DNA strand breaks is observed in activated cells only once they reach G_2/M. In summary, we show that the activated cells die by an apoptotic pathway after they reach G_2/M.

We next determined whether DNA synthesis was perturbed when synchronously cycling A11 cells are activated in early S phase. A11 cells were released from the drug block for ~1 h, and synchronously cycling early-S-phase cells were then collected by centrifugal elutriation. The progression of these cells into early S phase was monitored by flow cytometry. Using the incorporation of bromodeoxyuridine into DNA as a marker of DNA replication, we found that activated cells moved from early to mid- to late S phase indistinguishably from unactivated control cycling cells (Fig. 3A). These results suggest that DNA replication is not prematurely terminated when A11 cells are activated in the S phase. Immunofluorescence analysis revealed that condensation of chromatin, breakdown of nuclear lamin, and assembly of the mitotic spindle occurred equivalently in both activated cells and unactivated control cells as they entered mitosis (data not shown). By these criteria, A11 cells activated in the S phase enter mitosis. However, we observed two differences between activated cells in mitosis and control cells. First, in 60% of the activated cells the mitotic spindle failed to engage the chromosomes. In contrast, 90% of the unactivated control cells in mitosis displayed condensed chromosomes attached to a spindle. Second, MPM2 staining was greatly reduced in activated cells in mitosis, while control unactivated cells in mitosis stained intensely with MPM2 (Fig. 3B). The MPM2-specific monoclonal antibody recognizes a set of phosphorylated epitopes found predominantly in mitosis (6). Our results are consistent with the reported absence of MPM2 staining in murine thymocytes undergoing apoptosis (23). It therefore appears that events occurring during mitosis in synchronously cycling A11 cells after activation in the S phase are not normal. These abnormal events precede cell death, and cells with hypercondensed pycnotic nuclei and cytoplasmic blebbing become frequent 3 h after the mitotic peak and 8 h after activation of cells in the S phase (data not shown).

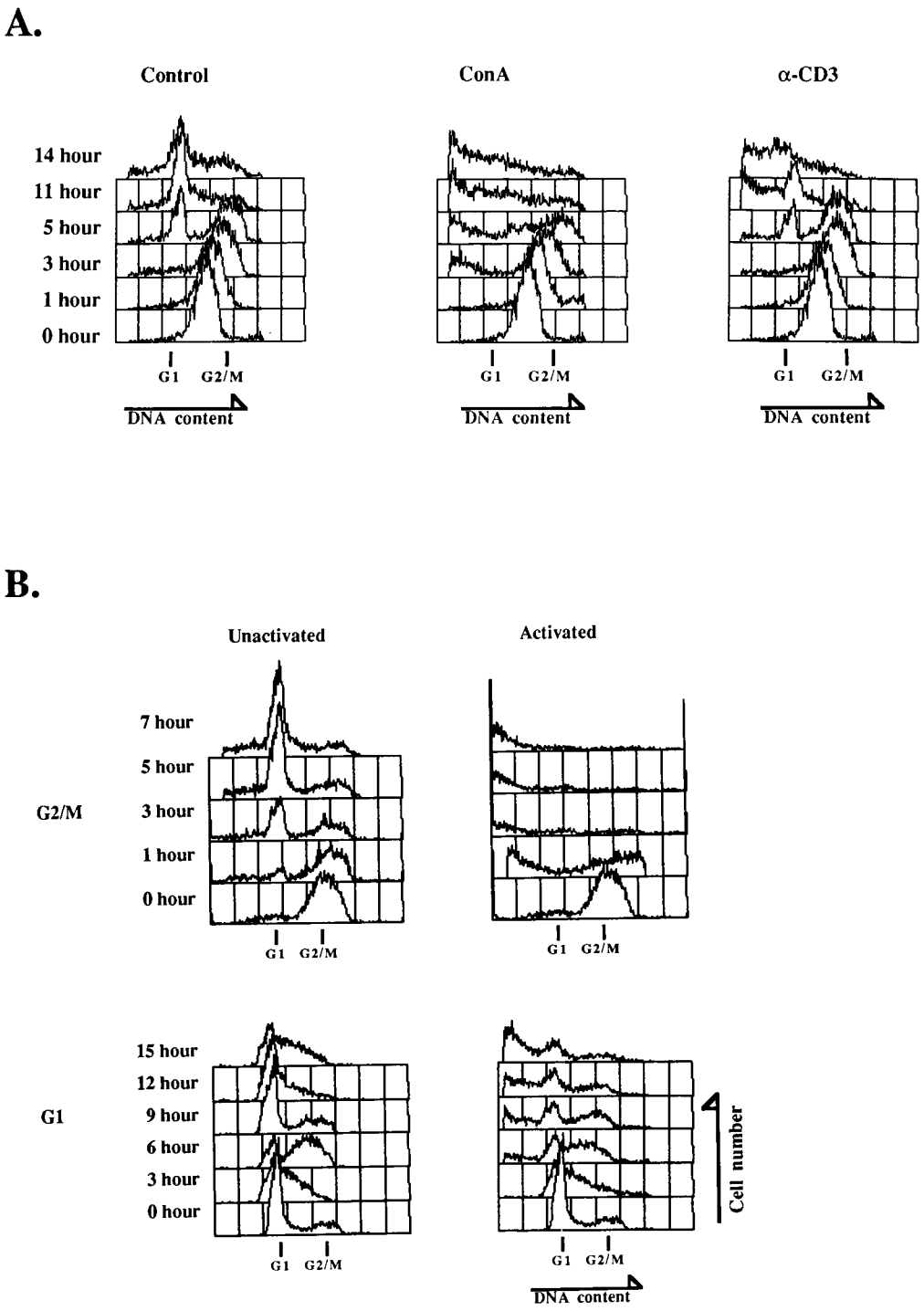

FIG. 1. Cell cycle progression of synchronously cycling T cells after activation at different phases of the cell cycle. (A) Cell cycle progression of synchronously cycling A11 cells activated in the S phase with ConA or anti-CD3 antibodies. Synchronously cycling A11 cells in the S phase were obtained after releasing A11 cells from an aphidicolin drug block and collecting S-phase cells by centrifugal elutriation. The DNA content of A11 cells was monitored from 0 to 14 h after activation and compared with that of control unactivated synchronously cycling cells. Cells containing less than G_1 DNA content appeared after control T cells entered G_2/M. (B) Cell cycle progression of A11 cells activated in G_2/M or G_1. Synchronously cycling A11 cells in G_2/M or G_1 were activated with ConA, and the DNA content was monitored at the indicated times after T-cell activation and compared with that of control unactivated cells. Synchronously cycling cells in G_2/M were obtained by releasing A11 cells from an aphidicolin drug block and collecting G_2/M-phase cells by centrifugal elutriation. Synchronously cycling cells in G_1 were obtained by centrifugal elutriation of asynchronous populations. Cells with less than G_1 DNA content appear after activated cells entered G_2/M. The viability of cells activated in G_2/M decreased to 20%, compared with 90% in unactivated synchronously cycling cells. The viability of cells activated in G_1 decreased to 30, compared with 95% in unactivated cycling cells.

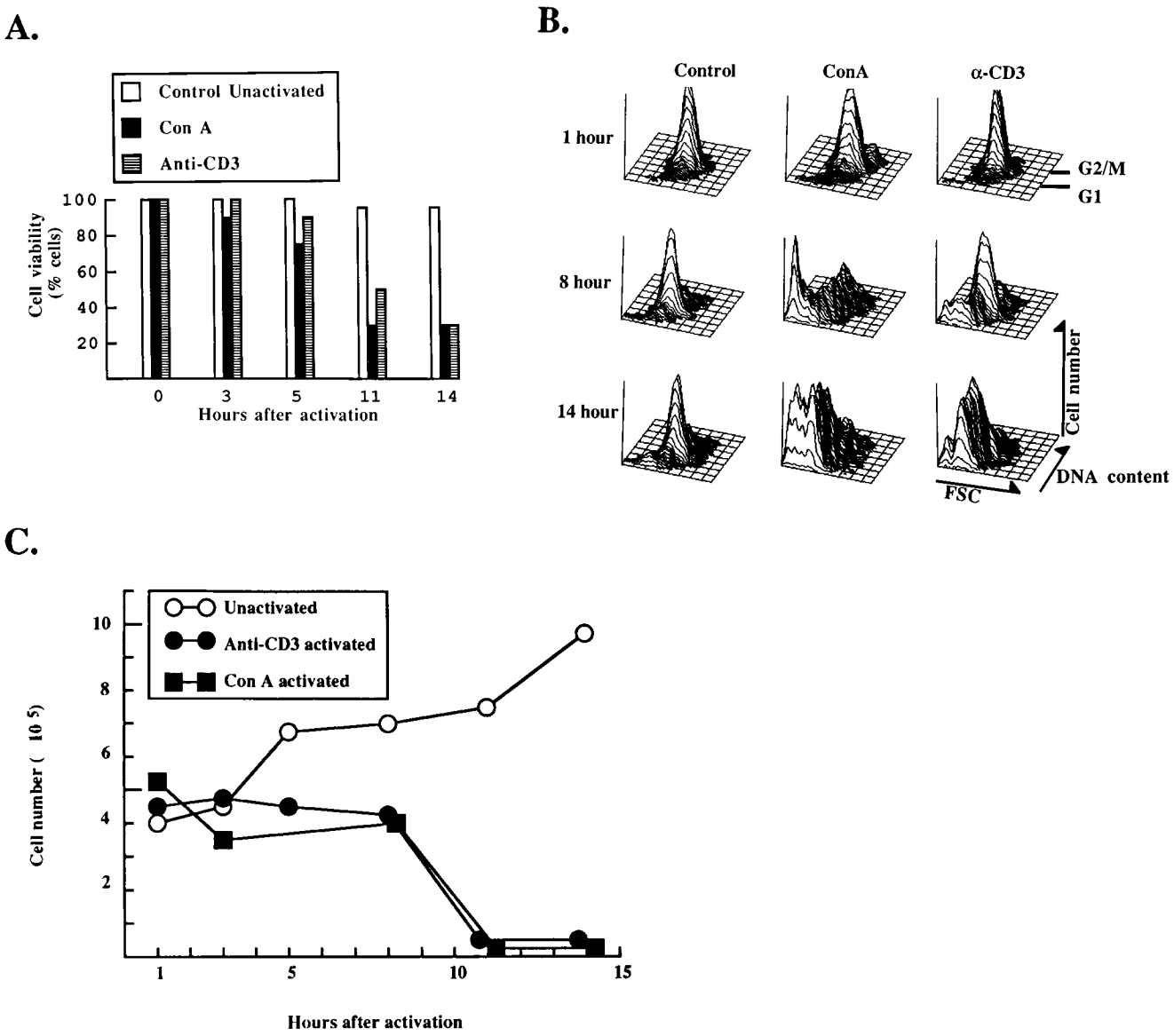

FIG. 2. Activation-induced cell death of synchronously cycling T cells activated in the S phase occurs after the cells reach G_2/M. The same cell populations analyzed in Fig. 1A were also subjected to analysis of cell viability and forward-angle scatter. (A) Activation-induced decrease in cell viability of activated T cells. Synchronously cycling A11 cells were activated in the S phase with either ConA or anti-CD3. Changes in cell viability were determined by trypan blue exclusion at various times after activation and compared with those of control unactivated cycling A11 cells. (B) Light-scattering properties of activated T cells. Synchronously cycling A11 cells in the S phase were activated with ConA or anti-CD3. The activated cells were analyzed for DNA content and forward-angle scatter at the indicated times after activation and compared with unactivated control cycling cells. The population with an aneuploid DNA content, induced after activation, had a low forward-angle scatter, indicative of apoptotic cell death (42, 46). (C) Synchronously cycling A11 cells do not divide after activation in the S phase. Synchronously cycling cells in the S phase were activated with either ConA or immobilized anti-CD3 antibodies. The total cell number (live plus dead) was determined at various times after activation with either ConA or anti-CD3 and compared with that of control unactivated synchronously cycling cells. Activated cells did not divide, whereas unactivated A11 cells doubled in number over the same period.

These results suggest that an inability to coordinate events in mitosis may be linked to the activation-induced cell death that occurs shortly after T cells reach G_2/M.

Histone H1 kinase activity is dramatically increased in T cells undergoing activation-induced cell death. To clarify whether perturbations of cell cycle regulators are coupled to activation-induced death of T cells, we assayed the histone H1 kinase activity associated with cyclin A, cyclin B1, and $p34^{cdc2}$ immunoprecipitates at various times after ConA activation of synchronous A11 cells in the S phase. As expected (7, 33), the control unactivated cells exhibit maximal levels of cyclin B- and $p34^{cdc2}$-associated H1 kinase activity in G_2/M, and the levels decline when cells enter G_1 (Fig. 4A). In contrast, the H1 kinase activity associated with both cyclins A and B and $p34^{cdc2}$ in extracts from activated cells was consistently higher than in extracts from unactivated cells (Fig. 4A). After activation, H1 kinase activity was elevated compared with that in unactivated cells in 10 different extracts and remained elevated (more than fourfold) at the time when unactivated cells exhibited a dramatic reduction of H1 kinase activity on reentry into G_1. The increase in H1 kinase activity was not due to an elevation of $p34^{cdc2}$ levels, since $p34^{cdc2}$, as determined by immunoblotting,

TABLE 1. Induction of DNA strand breaks by activation of synchronously cycling T cells in the S phase[a]

Activation and sampling time (h)	Cell cycle composition (% of cells)			% of cells with DNA strand breaks
	S	G_2/M	G_1	
Unactivated				
0	86	2	12	4
1	86	7	7	4
2	84	14	2	1
5	41	59	0	1
7	14	26	60	1
Activated				
1	84	10	6	14
2	74	26	0	39
5	48	52	0	60
7	35	64	1	76

[a] Synchronously cycling S-phase cells were obtained by releasing A11 cells from an aphidicolin drug block and collecting S-phase cells by centrifugal elutriation. These cells were then activated with ConA, the cell cycle composition was determined by propidium iodide staining (34), and DNA strand breaks were determined by the terminal transferase assay (15).

remained unchanged after T-cell activation (Fig. 4A). It is of interest that the induction of DNA strand breaks closely parallels the elevation in cyclin B-associated kinase activity after activation. Consistent with our observations in synchronously cycling A11 cells, we also found that ConA activation of asynchronous A11 cells caused a dramatic increase in cyclin B-associated H1 kinase activity, despite the fact that levels of $p34^{cdc2}$ and cyclin B remained unchanged in these asynchronous cells (Fig. 4B). Anti-CD3 activation of asynchronous A11 cells also induced $p34^{cdc2}$- and cyclin B-associated kinase activity ~threefold in three different extracts (Fig. 4C). The elevated levels of H1 kinase activity upon activation of T cells may explain why activated cells stop cycling.

The activity of $p34^{cdc2}$ is suppressed by phosphorylation on tyrosine 15 (31, 36), and specific dephosphorylation at this site activates entry into mitosis (8, 14, 35). We therefore determined the phosphotyrosine content of $p34^{cdc2}$ from activated and control unactivated cycling cells to assay the activation state of $p34^{cdc2}$. Although $p34^{cdc2}$ levels were unchanged after activation of an asynchronous population of A11 cells with ConA, $p34^{cdc2}$ was significantly dephosphorylated on tyrosine (Fig. 4B). Anti-CD3 activation of asynchronous A11 cells also

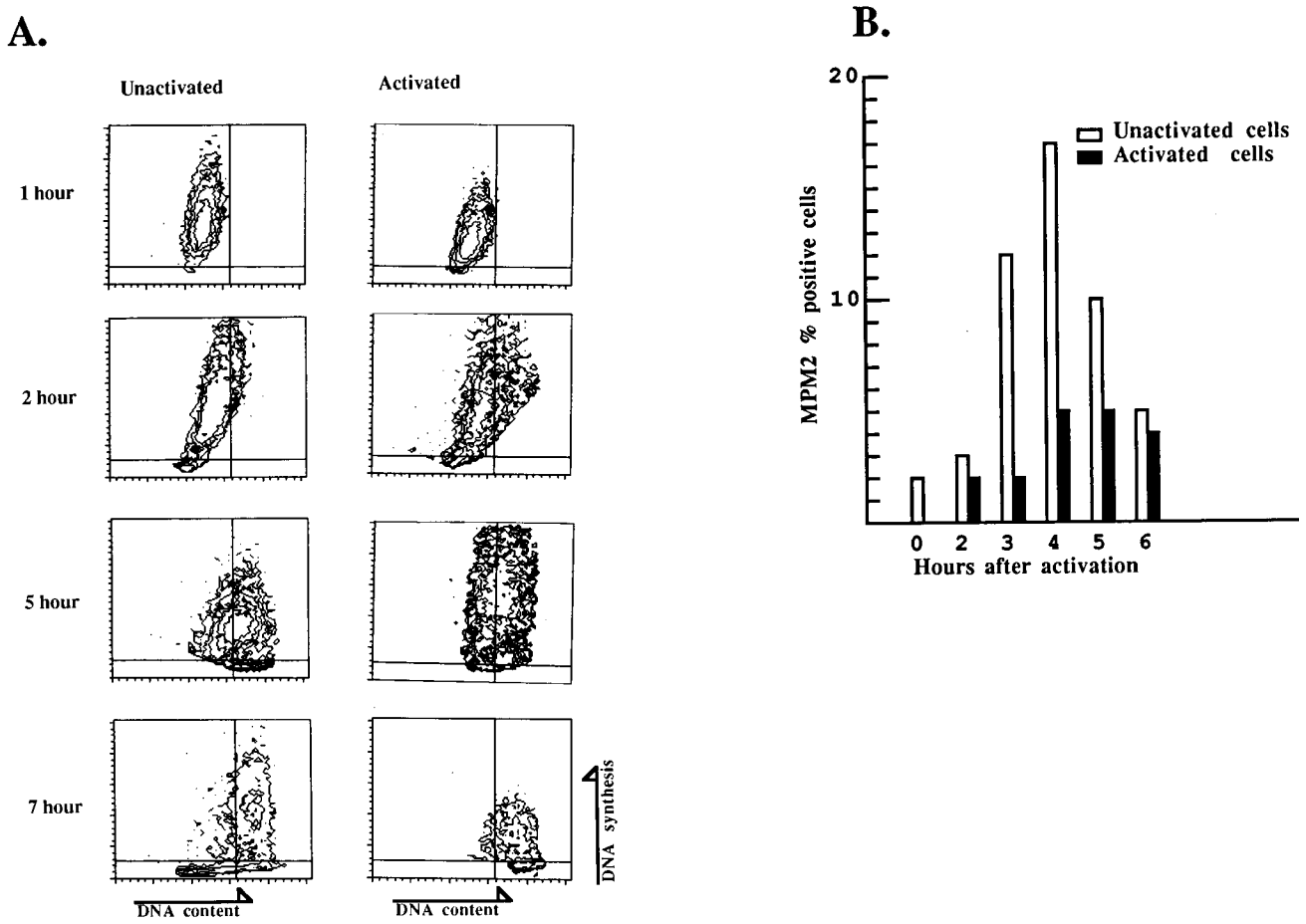

FIG. 3. Activation of synchronously cycling T cells in the S phase selectively perturbs cell cycle events in mitosis but not in the S phase. (A) DNA synthesis is not prematurely terminated after activation of A11 cells in early S phase. Synchronously cycling cells in early S phase were obtained as described in the text and activated with ConA. Cells were collected in parallel from activated and control unactivated A11 cells, at the indicated time after activation. DNA synthesis was monitored by estimating the incorporation of bromodeoxyuridine (29) and DNA content by propidium iodide staining (34). The ungated data demonstrated that both activated and unactivated A11 cells move from early to mid- to late S phase as demonstrated by this assay. Cells with less than G_1 content appear ~2 h after the end of DNA synthesis when A11 cells are activated in early S phase. (B) Expression of MPM2 antigen is greatly reduced in activated T cells. Synchronously cycling A11 cells in the S phase were activated with ConA. The percentage of activated cells which stained positive for MPM2 at the indicated times after activation was compared with that of unactivated synchronously cycling cells.

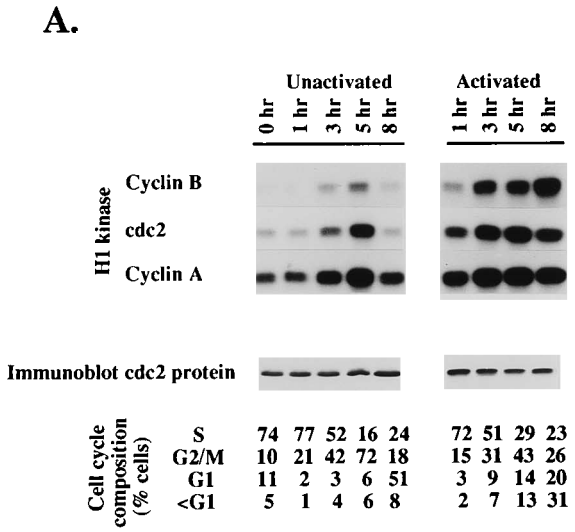

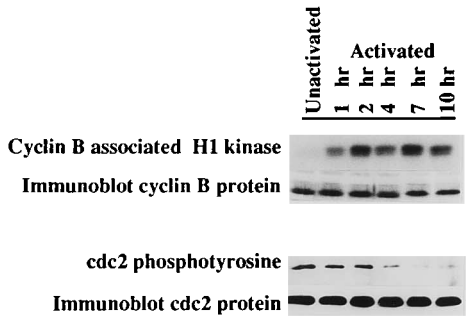

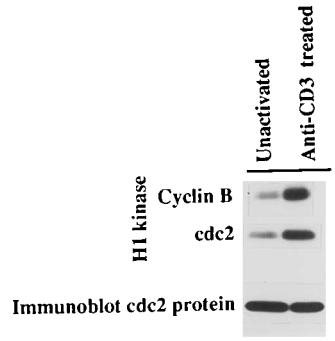

FIG. 4. Induction of elevated levels of histone H1 kinase activity after T-cell activation. (A) Elevation of H1 kinase activity by activation of synchronously cycling A11 cells in the S phase. Synchronous populations of A11 cells were activated in the S phase, and extracts were prepared at 0, 1, 3, 5, and 8 h from both unactivated and ConA-activated populations. Equal amounts of protein from both activated and unactivated cell extracts were immunoprecipitated with anti-cyclin B, anti-p34^{cdc2}, or anti-cyclin A antibodies. The immunoprecipitates were then assayed for histone H1 kinase activity. Equal amounts of protein from both activated and unactivated cell extracts were immunoblotted in parallel with anti-p34^{cdc2}-specific antibody. The cell cycle composition of the cells from which the extracts were made was determined by propidium iodide staining for DNA content. The percentages of cells in different phases of the cell cycle are shown. Similar results were obtained in experiments performed with 10 different extracts. (B) Elevation of H1 kinase activity and a decrease in the phosphotyrosine content of p34^{cdc2} after activation of asynchronous T cells. Cyclin B-associated H1 kinase activity of asynchronous A11 cells activated with ConA was determined as described in the legend to Fig. 2A. Equal amounts of protein from both activated and unactivated cell extracts were immunoblotted in parallel with anti-cyclin B or anti-p34^{cdc2} antibodies. p34^{cdc2} immunoprecipitates were analyzed for phosphotyrosine content in immunoblots with a phosphotyrosine-specific monoclonal antibody. (C) Elevation of H1 kinase activity after activation of asynchronous T cells with anti-CD3. Asynchronous A11 cells were activated with anti-CD3 for 10 h, and extracts were prepared from both activated and control unactivated cells. Cyclin B- and p34^{cdc2}-associated H1 kinase activity was determined as described for panel A.

TABLE 2. Induction of cell death by ectopic coexpression of cyclin B and p34^{cdc2}[a]

Plasmid	% of cells[b] with:		
	Signs of viability	<G_1 DNA content	DNA strand breaks
No DNA	100	9.6	1.8
CMV vector	100	13.2	9.5
Cyclin B	90	12.0	7.8
Cyclin B + p34^{cdc2}[c]	50	50.2	39.7

[a] Induction of cell death by coexpression of chicken p34^{cdc2} and a nondegradable form of chicken cyclin B (13, 22) in HeLa cells. The transfection efficiencies were ~30% as determined with a chicken cyclin B-specific antibody (13).

[b] The induction of cell death by transient transfection was monitored by several criteria: cell viability by trypan blue exclusion, DNA content by propidium iodide staining (34), and DNA strand breaks by the terminal transferase assay (15).

[c] The nondegradable cyclin B-p34^{cdc2} double transfections reproducibly induced cell death with three different plasmid preparations in six different experiments. Transient transfection with p34^{cdc2}-expressing plasmid did not induce cell death above vector background.

decreased the phosphotyrosine content of p34^{cdc2} (data not shown). These results suggest that tyrosine dephosphorylation of p34^{cdc2} parallels the increased levels of H1 kinase activity in T cells undergoing activation-induced cell death.

Induction of DNA fragmentation by ectopic expression of cyclin B and p34^{cdc2}. To determine if persistently elevated levels of cyclin B and p34^{cdc2} directly induce programmed cell death, a nondegradable (Arg-32 to Ser) form of cyclin B2 (22) was transiently coexpressed with p34^{cdc2} in HeLa cells (13). Using a chicken cyclin B2-specific antibody (13), we determined the transfection efficiency to be at least 30%. It should be noted that the actual number transfected may be larger, since the scoring of positive cells may be limited by the sensitivity of the chicken-specific antibody. Cell death was reproducibly induced in cell cultures cotransfected with both nondegradable cyclin B and p34^{cdc2}. The cell viability was reduced, and cell populations with less than G_1 DNA content and with DNA strand breaks were identifiable 48 h after cotransfection of cyclin B with p34^{cdc2}-expressing plasmids (Table 2). In experiments in which cells were doubly transfected with p34^{cdc2} and cyclin B, the increased induction of DNA strand breaks (30% of the total) over nonspecific background, as well as the increased appearance of cells with less than G_1 DNA content (37%), correlates reasonably well with the transfection efficiency of ~30%. These results suggest that coexpression of nondegradable cyclin B and p34^{cdc2} kinase can induce DNA strand breaks. Morphological examination also revealed that only cell cultures cotransfected with cyclin B and p34^{cdc2} exhibited cytoplasmic blebbing, a characteristic seen in apoptotic cell death. Cell cultures transfected with cyclin B alone or with the vector control did not exhibit cytoplasmic blebbing. Similar results were obtained by coexpression of degradable chicken B and p34^{cdc2} (data not shown). It is important to note that transfection with nondegradable cyclin B alone did not induce

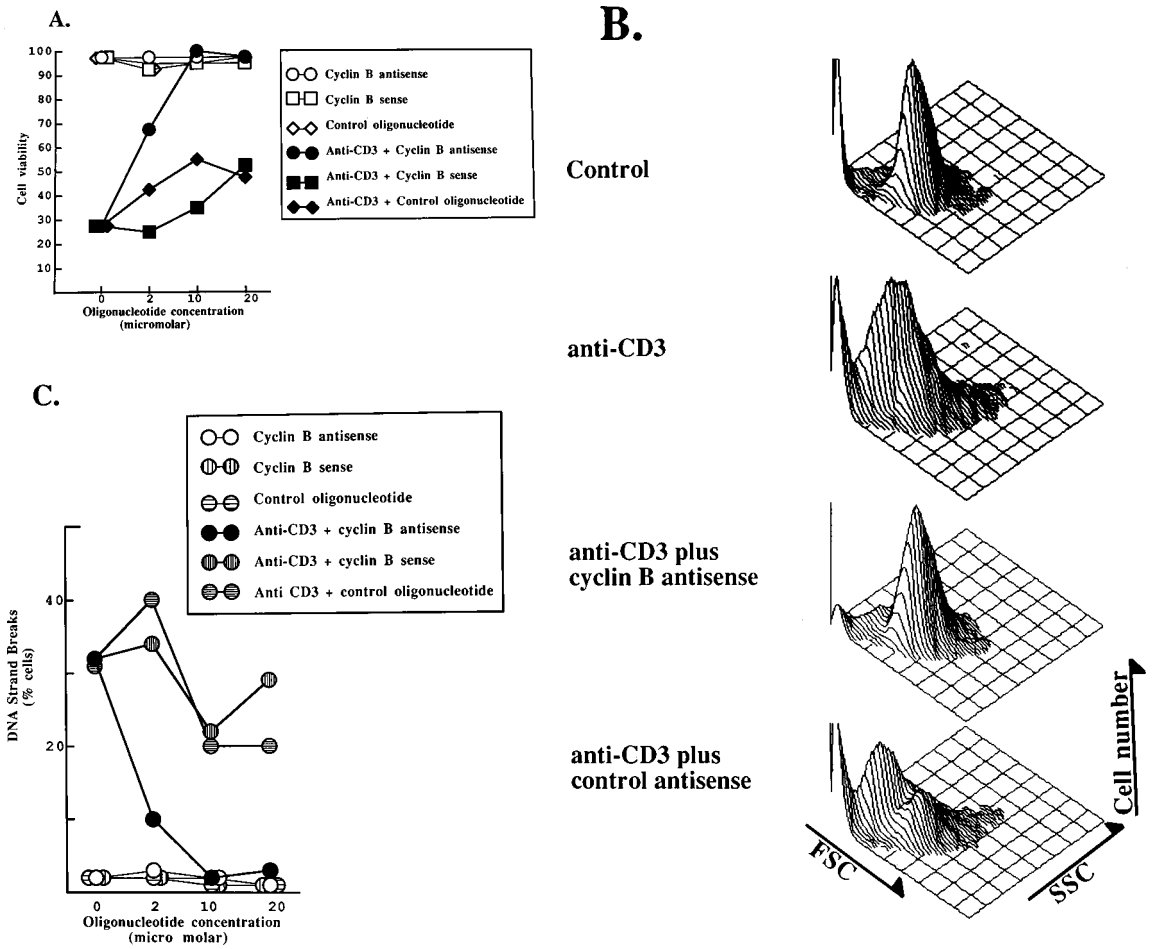

FIG. 5. Role of cyclin B-associated kinases in the induction of activation-induced programmed cell death. (A) Abrogation of anti-CD3-induced cell death in A11 cells by mouse cyclin B1-specific antisense phosphorothioate oligonucleotides. Asynchronous A11 cells were activated with anti-CD3 antibodies in the presence of cyclin B antisense, cyclin B sense, or control oligonucleotides at the indicated concentrations. The cell viability was determined by trypan blue exclusion 16 h after activation. The percentage of cyclin B-positive cells was reduced from 37 to 7% when A11 cells were grown with 20 μM cyclin B antisense oligonucleotide for 48 h. In contrast, ~30% of A11 cells grown with cyclin B sense or random control oligonucleotides were positive for cyclin B expression. (B) Cyclin B-specific antisense oligonucleotides completely inhibit anti-CD3-induced light-scattering changes characteristic of apoptotic A11 cells. Asynchronous A11 cells were activated with anti-CD3 for 16 h. Results shown are ungated data for forward-angle scatter (FSC) and side scatter (SSC). The data presented are for oligonucleotides at 2 μM. Identical results for the respective antisense oligonucleotides were obtained over a concentration range from 2 to 20 μM. (C) Anti-CD3-induced DNA strand breaks in A11 cells are abrogated by cyclin B-specific antisense oligonucleotides. Asynchronous A11 cells were activated with anti-CD3 antibodies in the presence of cyclin B antisense, cyclin B sense, or control oligonucleotide. The induction of DNA strand breaks by the terminal transferase assay (15) was determined 16 h after activation. The inhibition of DNA strand breaks induced after anti-CD3 activation of A11 cells by cyclin B antisense oligonucleotide was observed in eight separate experiments with five different batches of cyclin B antisense oligonucleotides.

cell death or DNA strand breaks but, as expected, induced mitotic arrest (13).

We also transiently cotransfected cyclin B and $p34^{cdc2}$ in C33A cells. C33A cells, unlike HeLa cells, express the cell surface marker CD20 after transfection with a CD20 expression plasmid. Double transfections with $p34^{cdc2}$ and cyclin B also consistently induced cell death (viability, ~50%) in C33A cells. When a cotransfection cell surface marker, CD20, was used, more than 80% of the CD20-positive cells died after double transfection with $p34^{cdc2}$ and cyclin B. In contrast, less than 20% of the CD20-positive cells died after transfection with either CD20 expression plasmid or CD20 plus cyclin B. We therefore conclude that cell death is specifically induced in cell cultures transiently cotransfected with $p34^{cdc2}$ and cyclin B.

Effect of cyclin B antisense oligonucleotides on activation-induced T-cell death. Cyclin B-specific antisense oligonucleotides were then used to determine if cyclin B expression is required for activation-induced programmed death of T cells. Our choice of the appropriate cyclin B1 antisense oligonucleotide was facilitated by the previous identification of antisense oligonucleotides which reproducibly abrogated cyclin B expression and maturation-promoting factor (MPF) activation (28). Antisense oligonucleotides corresponding to the equivalent region in murine cyclin B1 (32) were used to evaluate the role of cyclin B in anti-CD3-induced death of A11 cells. The effect of cyclin B antisense oligonucleotide on cyclin B expression in A11 cells was determined by immunofluorescence microscopy. The percentage of cyclin B-positive cells among A11 cells grown for 48 h in the presence of cyclin B antisense oligonucleotides was reduced from 37 to 7%. In contrast, ~30% of A11 cells grown with cyclin B sense or random control oligonucleotides were positive for cyclin B expression. A similar reduction in cyclin B-positive cells with cyclin B antisense but not cyclin B sense or random oligonucleotides was observed in three independent experiments.

Cyclin B antisense oligonucleotides dramatically reduced

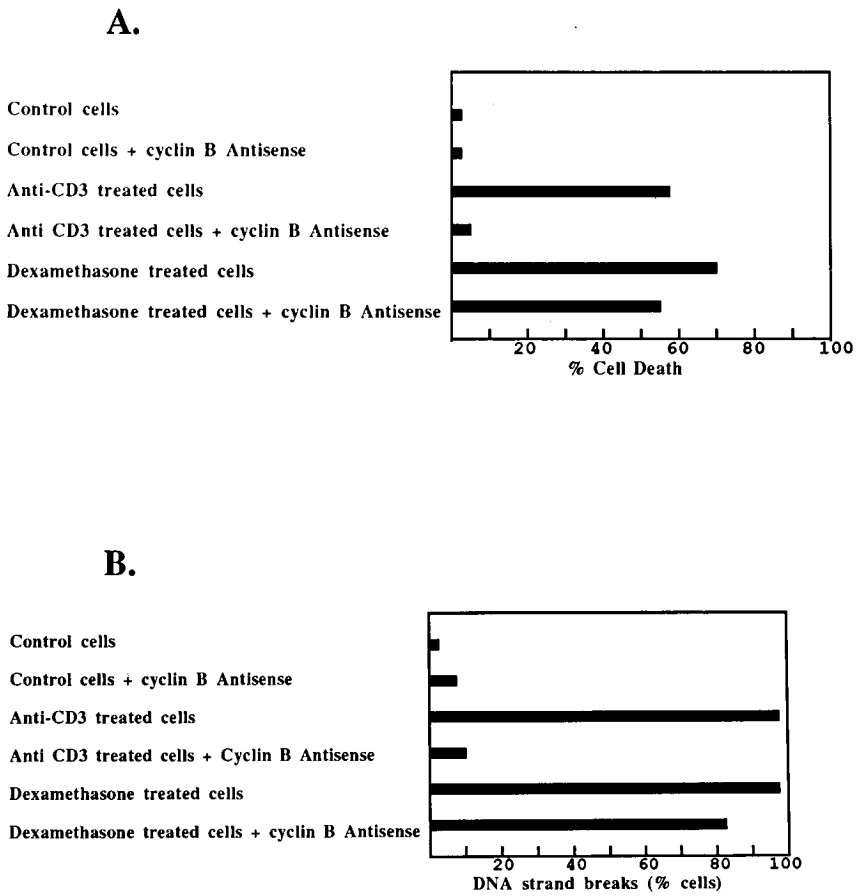

FIG. 6. Cyclin B antisense oligonucleotides do not inhibit dexamethasone-induced death of A11 cells. (A) Effect of cyclin B antisense oligonucleotides on dexamethasone-induced death of A11 cells. A11 cells were treated with 10^{-6} M dexamethasone in the presence or absence of 10 μM cyclin B antisense phosphorothioate oligonucleotides. Cell viability was determined by trypan blue exclusion after incubation of A11 for 16 h with dexamethasone. The data are shown as percent cell death (percentage of dead cells). (B) Effect of cyclin B antisense oligonucleotides on dexamethasone-induced DNA strand breaks in A11 cells. A11 cells were treated with 10^{-6} M dexamethasone in the presence or absence of 10 μM cyclin B antisense phosphorothioate oligonucleotides. DNA strand breaks were determined by the terminal transferase assay (15) after incubation of A11 for 16 h with dexamethasone.

anti-CD3-induced cell death in A11 cells, as demonstrated both by retention of cell viability (Fig. 5A) and by the absence of cells with less than G_1 DNA content (data not shown). In comparison, cyclin B sense oligonucleotide had no effect on anti-CD3-induced cell death (Fig. 5A). Similarly, a control random oligonucleotide with the same base composition as the cyclin B antisense oligonucleotide also did not inhibit activation-induced cell death (Fig. 5A). We also examined the morphological changes in A11 cells undergoing apoptosis, identifiable as a decrease in forward-angle light scatter (42, 46). This change was completely inhibited when cyclin B antisense oligonucleotide was added to anti-CD3-activated A11 cells (Fig. 5B). Anti-CD3-induced DNA strand breaks in A11 cells were also completely abrogated in the presence of cyclin B antisense oligonucleotide (Fig. 5C) in eight separate experiments. Cyclin B antisense oligonucleotide therefore suppresses anti-CD3-induced DNA strand breaks and loss of cell viability. We conclude that cyclin B is required for activation-induced cell death.

T-cell death can also be induced by other agents which do not activate T cells. Dexamethasone does not activate T cells but does induce programmed cell death (52), which is not dependent on either Myc (42) or proteases (37). We then examined if cyclin B antisense also inhibited cell death induced by dexamethasone. Dexamethasone-induced cell death, assayed by a decrease in cell viability and induction of DNA strand breaks, was not inhibited by cyclin B antisense oligonucleotide in A11 cells, whereas anti-CD3-induced cell death and DNA fragmentation were completely inhibited by the cyclin B antisense oligonucleotide (Fig. 6). The ability of cyclin B antisense oligonucleotide to inhibit anti-CD3-induced cell death is most probably due to specific downregulation of cyclin B. It is unlikely that this result is due to nonspecific inhibition of protein synthesis or the activation of a general cell survival receptor. Such nonspecific effects cannot explain the ability of cyclin B antisense oligonucleotide to inhibit anti-CD3-induced cell death but not dexamethasone-induced cell death in the same cell line. We therefore conclude that cyclin B is involved in anti-CD3-induced cell death.

DISCUSSION

We present a detailed study of perturbations in the cell cycle following activation of synchronously cycling cells. We have shown that activated A11 cells stop cycling after they reach G_2/M and subsequently undergo apoptotic cell death. The appearance of cells with less than G_1 DNA content, changes in cytoplasm as detectable by a decrease in forward-angle scatter, and induction of DNA strand breaks after activation all support the conclusion that cell death occurs by apoptosis. The

kinetics of onset of apoptosis, as determined by these criteria, supports our conclusion that cell death occurs after the cells reach G_2/M. The ability of synchronously cycling A11 cells to continue synthesizing DNA after activation in the S phase suggests that DNA synthesis is not terminated prematurely. This is also supported by a normal increase in DNA content in activated cells to levels seen in control cells in G_2/M. The breakdown of nuclear lamin and condensation of chromatin observed in activated A11 cells suggest that activated cells enter mitosis. However, the decreased expression of the MPM2 epitope and the failure of chromatin to associate with the mitotic spindle suggest that activated A11 cells go through an aberrant mitosis. The coincident increase in cyclin B- and $p34^{cdc2}$-associated kinase activity in activated cells further supports the idea that activated T cells undergoing programmed cell death fail to correctly coordinate mitotic events. It is therefore tempting to suggest that these aberrant mitotic events cause cell death.

The persistently elevated levels of cyclin B-associated kinase activity induced in activated T cells undergoing programmed cell death implicates cyclin B-associated kinase in the cell death mechanism. Our results are consistent with the increase in $p34^{cdc2}$ kinase activity observed in target cells which die because of apoptosis induced by a natural killer cell-specific protease (40). Our conclusion is further supported by our observation that DNA fragmentation can be induced in irrelevant cell types by co-overexpression of cyclin B with $p34^{cdc2}$. Our results are consistent with the fact that a mitotic catastrophe occurs when $p34^{cdc2}$ and cyclin B are overexpressed (18). The inhibition of anti-CD3-induced DNA strand breaks and cell death in A11 cells by a cyclin B-specific antisense oligonucleotide further implicates cyclin B-associated kinase in cell death. In contrast, the cyclin B antisense oligonucleotide fails to inhibit dexamethasone-induced death of A11 cells. These results suggest that there are at least two apoptosis death pathways: one which is dependent on activation through surface receptors (ConA or anti-CD3), leading to cyclin B-dependent cell death during G_2/M, and another (such as the dexamethasone-induced pathway) which is independent of cell activation and cyclin B. It is of interest that protease inhibitors block anti-CD3-induced cell death but not dexamethasone-induced cell death (37).

The ability of cyclin B-associated kinase activity to induce cell death suggests that proteins phosphorylated by this kinase can act as mediators of cell death. One such potential target of cyclin B kinase in apoptotic cell death is c-Myc. Firstly, c-Myc has been implicated in activation-induced cell death (42). Second, phosphorylation of c-Myc at Ser-62 is critical for transactivation (38), and this residue is preferentially phosphorylated during G_2/M (38). In our model system, T-cell activation increases the ability of cyclin B kinase to phosphorylate c-Myc at Ser-62 by two- to fivefold (10a). It is of interest that both cyclin B antisense oligonucleotide (this work) and c-Myc antisense oligonucleotide (42) abrogate anti-CD3-induced cell death but not dexamethasone-induced cell death (43; also see above).

It is not yet clear if activation via the T-cell receptor stimulates cyclin B-associated kinase directly or through an indirect effect on a regulator of cyclin B kinase activity. It has been previously reported that the Wee1 kinase regulates phosphorylation of $p34^{cdc2}$ at Tyr-15, inactivating kinase activity (31, 36) of activated $p34^{cdc2}$, whereas Cdc25 dephosphorylates $p34^{cdc2}$ on Tyr-15 and activates kinase activity (8, 14, 35). The persistent elevation of cyclin B-associated kinase activities could be caused by the inactivation of Wee1 or by inappropriate and persistent induction of Cdc25 in T cells undergoing activation induced cell death. Alternatively, persistent elevation of cyclin B-associated kinase activity could be caused by inhibition of cyclin B degradation. Our data on tyrosine dephosphorylation of $p34^{cdc2}$ support a role for Wee1/Cdc25 deregulation. More direct experiments will now be required to define the mechanism underlying elevation of cyclin B-associated kinase activity and the role of this activation in inducing cell death.

ACKNOWLEDGMENTS

We acknowledge the kind gift of chicken $p34^{cdc2}$ and cyclin B plasmids and antibodies from Eric A. Nigg, Epalinges, Switzerland, and the CD20 expression plasmid from S. van den Heuvel and E. Harlow, Charlestown, Mass. We thank Sheila Erickson (Grenoble) and Howard Brickner (La Jolla) for technical assistance and Doug Green for discussions.

This work was supported by American Cancer Society grant DB107 and institutional funds to A.F. and by grants from CNRS, INSERM (grant 508101), and ARC (grant 6657) to R.F.

REFERENCES

1. **Andreassen, P. R., and R. L. Margolis.** 1991. Induction of partial mitosis in BHK cells by 2-aminopurine. J. Cell Sci. **100:**299–310.
2. **Ashwell, J. D., R. E. Cunningham, P. Noguchi, and D. Hernandez.** 1987. Cell growth cycle block of T cell hybridomas upon activation with antigen. J. Exp. Med. **165:**173–194.
3. **Bluestone, J. A., D. Pardoll, S. O. Sharrow, and B. Folkes.** 1987. Characterization of murine thymocyte CD3-associated T cell receptor structures. Nature (London) **326:**82–84.
4. **Breitmayer, J. B., S. O. Oppenheim, J. F. Daley, H. B. Levine, and S. F. Schlossman.** 1987. Growth inhibition of human T cells by antibodies recognizing the T cell antigen receptor complex. J. Immunol. **139:**726–731.
5. **Clarke, A. R., C. Purdie, D. Harrison, R. Morris, C. C. Bird, M. L. Hooper, and A. H. Wyllie.** 1993. Thymocyte apoptosis induced by p53-dependent and independent pathways. Nature (London) **362:**849–852.
6. **Davis, F. M., T. Y. Tsao, S. K. Fowler, and P. N. Rao.** 1983. Monoclonal antibodies to mitotic cells. Proc. Natl. Acad. Sci. USA **80:**2926–2930.
7. **Draetta, G., and D. Beach.** 1988. Activation of $p34^{cdc2}$ protein kinase during mitosis in human cells: cell cycle dependent phosphorylation and subunit rearrangement. Cell **54:**17–26.
8. **Dunphy, W. G., and A. Kumagai.** 1991. The cdc25 protein contains an intrinsic phosphatase activity. Cell **67:**189–196.
9. **Evan, G. I., A. H. Wyllie, C. S. Gilbert, T. D. Littlewood, H. Land, M. Brooks, C. Waters, L. Z. Penn, and D. C. Hannock.** 1992. Induction of apoptosis in fibroblasts by c-myc protein. Cell **69:**119–128.
10. **Fotedar, A., M. Boyer, W. Smart, J. Widtman, E. Fraga, and B. Singh.** 1985. Fine specificity of antigen recognition by T cell hybridomas clones specific for poly-18: a synthetic polypeptide of defined sequence and conformation. J. Immunol. **135:**3028–3033.

10a. **Fotedar, R., and A. Fotedar.** Unpublished data.

11. **Fotedar, R., and J. M. Roberts.** 1991. Association of $p34^{cdc2}$ with the replication initiation complex. Cold Spring Harbor Symp. Quant. Biol. **56:**325–333.
12. **Fotedar, R., and J. M. Roberts.** 1992. Cell cycle regulated phosphorylation of RPA-32 occurs within the replication initiation complex. EMBO J. **11:**2177–2187.
13. **Gallant, P., and E. A. Nigg.** 1992. Cyclin B2 undergoes cell cycle dependent nuclear translocation and when expressed as a nondestructible mutant causes mitotic arrest in HeLa cells. J. Cell Biol. **117:**213–224.
14. **Gautier, J., M. J. Solomon, R. Booher, J. F. Bazan, and M. W. Kirschner.** 1991. cdc25 is a specific tyrosine phosphatase that directly activates $p34^{cdc2}$. Cell **67:**197–211.
15. **Gorczyca, W., J. Gong, and Z. Darzynkiewicz.** 1993. Detection of DNA strand breaks in individual apoptotic cells by the in situ terminal deoxynucleotidal transferase and nick translation assays. Cancer Res. **52:**1945–1951.
16. **Guadagno, T. M., M. Ohtusbo, J. M. Roberts, and R. K. Assoian.** 1993. A link between cyclin A expression and adhesion dependent cell cycle progression. Science **262:**1572–1575.
17. **Guilly, M. N., F. Danon, J. C. Brouet, M. Bornens, and J. C. Courvalin.** 1987. Autoantibodies to nuclear lamin B in a patient with thrombopenia. Eur. J. Cell Biol. **43:**266–272.
18. **Heald, R., M. McLoughlin, and F. McKeon.** 1993. Human Wee1 maintains mitotic timing by protecting the nucleus from cytoplasmic activated $p34^{cdc2}$ kinase. Cell **74:**463–474.
19. **Hengartner, M. O., R. E. Ellis, and H. Horowitz.** 1992. Caenorhabditis elegans gene ced-9 protects cells from programmed cell death. Nature (London) **356:**494–499.
20. **Hockenbery, D., G. Nunez, C. Milliman, R. D. Schreiber, and S. J. Korsmeyer.** 1990. Bcl-2 is an inner mitochondrial membrane protein that blocks programmed cell death. Nature (London) **348:**334–336.

21. **Jenkinson, E. J., R. Kingston, C. A. Smith, G. T. Williams, and J. J. T. Owen.** 1989. Antigen induced apoptosis in developing cells a mechanism for negative selection of the T cell receptor repertoire. Eur. J. Immunol. **19:**2175–2177.
22. **Krek, W., and E. A. Nigg.** 1991. Mutations of p34^{cdc2} phosphorylation sites induce premature mitosis in HeLa cells: evidence for a double block to p34^{cdc2} kinase activation in vertebrates. EMBO J. **10:**3331–3341.
23. **Lazebnik, Y. A., S. Cole, C. A. Cooke, W. G. Nelson, and W. C. Earnshaw.** 1993. Nuclear events of apoptosis in cell free mitotic extracts: a model system for analysis of the active phase of apoptosis. J. Cell Biol. **123:**7–22.
24. **Liu, Z.-G., S. Smith, K. A. McLaughlin, L. M. Schwartz, and B. A. Osborne.** 1994. Apoptotic signals delivered through the T-cell receptor of a T cell hybrid require the immediate early gene nur77. Nature (London) **367:**281–284.
25. **McConkey, D. J., P. Hartzell, J. F. Amadar-Perez, S. Orrenius, and M. Jondal.** 1989. Calcium dependent killing of immature thymocytes by simulation via the CD3/T cell receptor complex. J. Immunol. **143:**1801–1806.
26. **Mercep, M., J. A. Bluestone, P. Nogucji, and J. D. Ashwell.** 1988. Inhibition of transformed T cell growth invitro by monoclonal antibodies directed against activating molecules. J. Immunol. **140:**324–335.
27. **Mercep, M., P. Noguchi, and J. D. Ashwell.** 1989. The cell cycle block and lysis of an activated T cell hybridoma are distinct processes with different Ca^{++} requirements and sensitivity to cyclosporine A. J. Immunol. **142:**4085–4092.
28. **Minshull, J., J. J. Blow, and T. Hunt.** 1989. Translation of cyclin B mRNA is necessary for extracts of activated Xenopus eggs to enter mitosis. Cell **56:**947–956.
29. **Nau, G. J., D.-K. Kim, and F. W. Fitch.** 1988. Agents that mimic antigen receptor signalling inhibit proliferation of cloned murine T lymphocytes induced by IL2. J. Immunol. **141:**3557–3563.
30. **Oltvai, Z. N., C. L. Milliman, and S. J. Korsmeyer.** 1993. Bcl2 heterodimerises in vivo with a conserved homolog Bax that accelerates programmed cell death. Cell **74:**609–620.
31. **Parker, L. L., and H. Piwnica-Worms.** 1992. Inactivation of the p34^{cdc2}-cyclin B complex by the human WEE1 tyrosine kinase. Science **257:**1955–1957.
32. **Paterno, G. D., and K. M. Downs.** 1991. Sequence of a cDNA encoding a mouse cyclin B protein. Gene **108:**315–316.
33. **Pines, J., and T. Hunter.** 1989. Isolation of a human cyclin cDNA: evidence for cyclin mRNA and protein regulation in the cell cycle and for interaction with p34^{cdc2}. Cell **58:**833–846.
34. **Robinson, J. P. (ed.).** 1993. Handbook of flow cytometry methods. Wiley-Liss, New York.
35. **Russell, P., and P. Nurse.** 1986. cdc25C^{+} functions as an inducer in the mitotic control of fission yeast. Cell **45:**145–153.
36. **Russell, P., and P. Nurse.** 1987. Negative regulation of mitosis by wee1^{+} a gene encoding a protein kinase homolog. Cell **49:**559–567.
37. **Sarin, A., D. H. Adams, and P. A. Henkart.** 1993. Protease inhibitors selectively block T cell receptor triggered programmed cell death in a murine T cell hybridoma and activated peripheral T cells. J. Exp. Med. **178:**1693–1700.
38. **Seth, A., S. Gupta, and R. J. Davis.** 1993. Cell cycle regulation of the c-Myc transcriptional domain. Mol. Cell. Biol. **13:**4125–4136.
39. **Sherwood, S. W., A. L. Kung, J. Roitelman, R. D. Simoni, and R. T. Schimke.** 1993. In vivo inhibition of cyclin B degradation and induction of cell cycle arrest in mammalian cells by the neutral cysteine protease inhibitor N-acetylleucylleucylnorleucinal. Proc. Natl. Acad. Sci. USA **90:**3353–3357.
40. **Shi, L., W. K. Nishioka, J. Th'ng, E. M. Bradbury, D. W. Litchfield, and A. H. Greenberg.** 1994. Premature p34^{cdc2} activation required for apoptosis. Science **263:**1143–1145.
41. **Shi, Y., R. P. Bissonnette, N. Parfrey, M. Szalay, R. T. Kubo, and D. G. Green.** 1991. In vivo administration of antibodies to the CD3/T cell receptor complex induces cell death (apoptosis) in immature thymocytes. J. Immunol. **146:**3340–3348.
42. **Shi, Y., J. M. Glynn, L. J. Guilbert, T. G. Cotter, R. P. Bissonnette, and D. R. Green.** 1992. Role of c-myc in activation induced apoptotic cell death in T cell hybridomas. Science **257:**212–214.
43. **Shi, Y., B. Sahai, and D. R. Green.** 1989. Cyclosporin A inhibits activation induced cell death in T cell hybridomas and in thymocytes. Nature (London) **339:**625–626.
44. **Shi, Y., M. Szalay, L. Paskar, B. Sahai, M. Boyer, B. Singh, and D. G. Green.** 1990. Activation induced cell death in T cell hybridomas is due to apoptosis: morphological aspects and DNA fragmentation. J. Immunol. **145:**3326–3333.
45. **Smith, C. A., G. Williams, R. Kingston, E. Jenkinson, and J. J. Owen.** 1989. Antibodies to CD3/T cell receptor complex induced by apoptosis in immature T cells in thymic cultures. Nature (London) **337:**181–184.
46. **Swat, W., L. Ignatowicz, and P. Kisielow.** 1991. Detection of apoptosis of immature CD4+8+ thymocytes by flow cytometry. J. Immunol. Methods **137:**79–87.
47. **Tadakuma, T., H. Kizaki, C. Odaka, R. Kubota, Y. Ishimura, H. Yagita, and K. Okumura.** 1990. CD4+CD8+ thymocytes are susceptible to DNA fragmentation induced by phorbol esters, calcium ionophore and anti-CD3 antibody. Eur. J. Immunol. **20:**779–784.
48. **Webb, S., and J. Sprent.** 1987. Downregulation of T cell responses by antibodies to the T cell receptor. J. Exp. Med. **165:**584–589.
49. **Woronicz, J. D., B. Calnan, V. Ngo, and A. Winoto.** 1994. Requirement of the orphan steroid receptor Nur77 in apoptosis of T cell hybridomas. Nature (London) **367:**277–281.
50. **Wyllie, A. H., J. F. R. Kerr, and A. R. Currie.** 1980. Cell death: the significance of apoptosis. Int. Rev. Cytol. **68:**251–305.
51. **Yuan, J., S. Shaham, S. Ledouux, H. M. Ellis, and H. Horvitz.** 1993. The C. elegans cell death gene ced-3 encodes a protein similar to mammalian interleukin-1β-converting enzyme. Cell **75:**641–652.
52. **Zacharchuk, C. M., M. Mercep, P. K. Chakaraborti, S. S. Simons, and J. D. Ashwell.** 1990. Programmed T lymphocyte death: cell activation and steroid induced pathways are mutually antagonistic. J. Immunol. **145:**4037–4045.